

Enhanced green laser activation by antireflective gate structures in panel transistors

Jia-Min Shieh, Chih Chen, Yu-Ting Lin, and Ci-Ling Pan

Citation: *Applied Physics Letters* **92**, 063503 (2008); doi: 10.1063/1.2842417

View online: <http://dx.doi.org/10.1063/1.2842417>

View Table of Contents: <http://scitation.aip.org/content/aip/journal/apl/92/6?ver=pdfcov>

Published by the [AIP Publishing](#)

Articles you may be interested in

[Characteristics and stress-induced degradation of laser-activated low temperature polycrystalline silicon thin-film transistors](#)

J. Appl. Phys. **93**, 1926 (2003); 10.1063/1.1535732

[Thermal oxide of polycrystalline silicon on steel foil as a thin-film transistor gate dielectric](#)

Appl. Phys. Lett. **78**, 3729 (2001); 10.1063/1.1377319

[Erratum: "Effect of excimer laser annealing on the structural and electrical properties of polycrystalline silicon thin-film transistors" \[*J. Appl. Phys.* 86, 4600 \(1999\)\]](#)

J. Appl. Phys. **87**, 1588 (2000); 10.1063/1.372060

[Effect of excimer laser annealing on the structural and electrical properties of polycrystalline silicon thin-film transistors](#)

J. Appl. Phys. **86**, 4600 (1999); 10.1063/1.371409

[Electrical and noise properties of thin-film transistors on very thin excimer laser annealed polycrystalline silicon films](#)

Appl. Phys. Lett. **74**, 3684 (1999); 10.1063/1.123221



NEW! Asylum Research MFP-3D Infinity™ AFM
Unmatched Performance, Versatility and Support

OXFORD INSTRUMENTS
The Business of Science®

Stunning high performance

Simpler than ever to GetStarted™

Comprehensive tools for nanomechanics

Widest range of accessories for materials science and bioscience

Asylum Research

Enhanced green laser activation by antireflective gate structures in panel transistors

Jia-Min Shieh,^{1,2,a)} Chih Chen,^{3,b)} Yu-Ting Lin,³ and Ci-Ling Pan²

¹National Nano Device Laboratories, Hsinchu 30078, Taiwan

²Department of Photonics and Institute of Electro-Optical Engineering, National Chiao Tung University, Hsinchu 30010, Taiwan

³Department of Material Science and Engineering, National Chiao Tung University, Hsinchu 30010, Taiwan

(Received 12 December 2007; accepted 21 January 2008; published online 13 February 2008)

Antireflective gate structures of polycrystalline silicon (poly-Si) and silicon dioxide films enable postimplantation green continuous-wave laser annealing of all Si regions of green laser-crystallized panel Si transistors. About 40% of the incident laser-energy penetrates to the channels, owing to antireflective gate structures with the absorptive gate poly-Si, while 65% of the incident laser-energy enters the source/drain regions because of Fresnel reflections at the air/source (drain) interfaces. Such inverted laser-energy profiles and ascendant defect distributions along the channels/junctions/contact regions, yielded continuous, improved epilike Si microstructures over the entire active layer. The electron mobility of the transistors, $620 \text{ cm}^2/\text{V s}$, approaches that of integrated-circuits transistors. © 2008 American Institute of Physics. [DOI: 10.1063/1.2842417]

High-performance polycrystalline silicon thin-film transistors (poly-Si TFTs) on glass substrates increasingly influence prophetic circuits¹ and current drivers. A high-speed and reliable transistor must have a thin channel. The increase in the parasitic source/drain (S/D) resistance by shrinkage of the channel layer is normally reduced by the introduction of SiGe-raised S/D (Ref. 2) structures or by applying advanced activation techniques. Temperature constrains the activation of S/D junctions in several transistors, including panel transistors³ and integrated-circuit transistors with Ge channels and high- κ gate dielectrics⁴ or shallow junctions.⁵ Hence, thermal annealing technologies must continue to advance. Dopant activation by ultraviolet (UV), green,⁶ and near-infrared⁷ laser-irradiation of S/D regions has been demonstrated in the fabrication of transistors. However, laser activation, unlike laser crystallization, generates discontinuities⁸ and/or residual damage⁹ in microstructures across junctions because of variations in the laser energy that is scanned over the device bodies, which are formed from the gate (G) structures.

With reference to panel applications, in backside laser activation, the percentage of laser energy that was scanned into the channels equaled that scanned into the S/D regions and junctions. Although the numbers of defects varied among the channels, junctions, and contact regions, formation of improved channel microstructures over the entire channel/junction demonstrated and explained the enhanced mobility and reliability of the panel epilike silicon transistors using backside green laser activation.⁶ The fact that the absorbed fraction of light energy in irradiated poly-Si layers substantially declines as the laser wavelength increases¹⁰ supports the claim that gate structures of poly-Si and dielectric SiO₂ films as double-layer antireflectors¹¹ promote the transmission of front-side green laser irradiation to channels by as much as 40%, while 65% of the incident laser energy enters the S/D regions because of air/S (D) poly-Si Fresnel

reflection. Such inverted laser-energy profiles together with ascendant defect distributions along channels/junctions/contact region form continuous improved epilike Si microstructures over the entire channel/junction and low parasitic source/drain resistance.

This study explores antireflective gate structures to enhance front-side green continuous-wave (cw) laser activation (CLA) in panel transistors on green cw laser-crystallized epilike Si layers.

Poly-Si channels on quartz substrates were formed by the green cw laser crystallization (CLC) (laser energy of $\sim 4.2 \text{ W}$) of amorphous silicon islands with thickness of 100 nm, which were deposited by plasma-enhanced chemical vapor deposition (PECVD). Gate dielectrics of PECVD SiO₂, with a thickness of 115 nm together with thermally deposited poly-Si gates with a thickness of 250 nm, are applied to form self-aligned transistors. Poly-Si gates and S/D regions were doped with PH₃ ($5.0 \times 10^{15} \text{ cm}^{-2}$ and 25 keV) and activated by furnace thermal annealing (FA) for 12 h at 580 °C or green cw laser irradiation at 2.2–2.8 W. The parasitic S/D resistance of laser (FA)-activated TFTs was determined from the relationship between the channel-width ($W=10 \mu\text{m}$)-normalized on resistance (R_{on}) (Ref. 12) and the length of the channel ($L=5-15 \mu\text{m}$). The grain trap-state densities n_{GT} of TFTs were examined using the field-effect conductance method.¹³

Figure 1(a) plots the simulated transmittance spectrum of incident light across the gate structures of poly-Si/SiO₂ toward the channels. The visible (450–800 nm) transmittance spectrum exhibits a pattern of interference fringes with transmittance that fluctuates between 10% and 60% because of the gate structures and the considerably long penetration depth of visible light in poly-Si gates.¹⁰ In front-side green laser irradiation, up to 40% of the incident laser energy enters the channels, enough to recrystallize a few small grains in the channels, as indicated by the n_{GT} of the green laser-activated devices between the tail and the middle energetic levels (E) that were far from the Fermi level (E_F), such that, $\Delta E = E - E_F = 0.5 - 0.35 \text{ eV}$, which decreases markedly as the

a)Electronic mail: jmshieh@ndl.org.tw; jmshieh@faculty.nctu.edu.tw.

b)Electronic mail: chih@faculty.nctu.edu.tw.

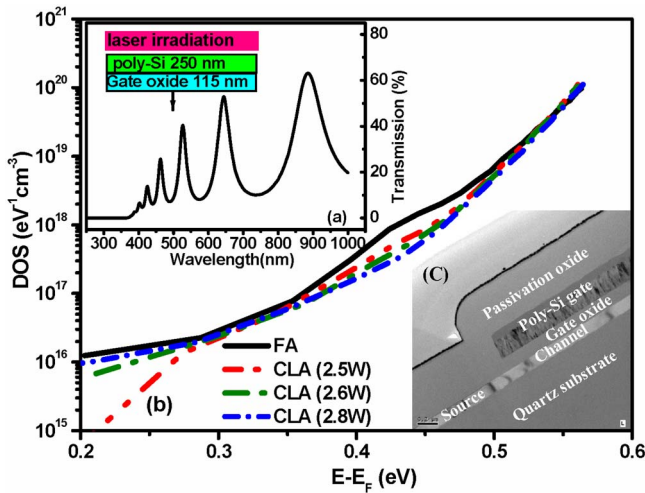


FIG. 1. (Color online) (a) Simulated transmittance spectrum for incident light through gate structures to channels. (b) Energy distribution associated with grain trap-state densities in TFTs that were made on CLC poly-Si and activated by FA and front-side green laser irradiation at 2.5–2.8 W. (c) Cross-sectional transmission electron microscopic image of representative laser-activated TFT.

laser-activation energy increases [Fig. 1(b)]. Moreover, the tail-state density of grain traps measured in green laser-activated devices, which was closely related to channel crystallinity,^{14,15} n_{GT} at $\Delta E = E - E_F = 0.56 - 0.5$ eV, was independent of laser-activation energy and identical to that measured in FA-activated devices [Fig. 1(b)].

Fresnel reflection at air/S (D) interfaces causes 65% of the incident green laser-activation energy to enter the S/D region, which sufficed to repair these regions that were amorphized by implantation.¹⁶ Parasitic S/D resistance that was determined by merging numerous curves of $R_{on}(V_g)$ against L (Ref. 12) for green laser-activated TFTs gradually fall and saturate at 1.9 k Ω as the incident laser energy increases to 2.8 W [Figs. 2(a)–2(c)]. This value is close to the value 1.8 k Ω for FA-activated TFTs [Fig. 2(d)]. Gate antireflectors ensure that the laser energy penetrates into channels and improves the channel microstructures with fewer grain defects [Fig. 1(b)]. Furthermore, postimplantation thermal annealing hardly improves channel microstructures even though it re-

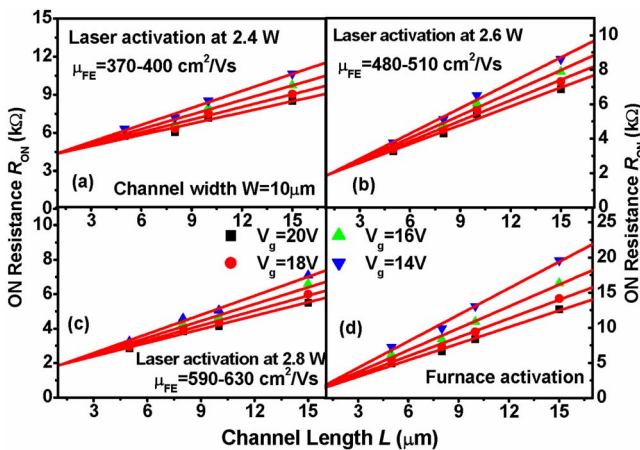


FIG. 2. (Color online) Channel width-normalized resistance of TFTs that were made on CLC poly-Si and activated by front-side green laser irradiation at (a) 2.4 W, (b) 2.6 W, and (c) 2.8 W, as well as by (d) FA vs channel length.

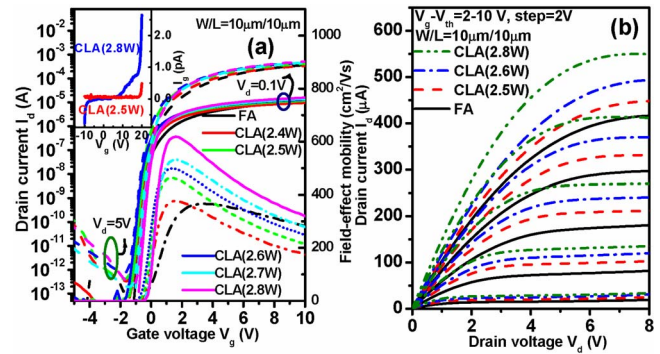


FIG. 3. (Color online) (a) Transfer characteristics (taken at $V_d = 5$ and 0.1 V) and transconductance curves (taken at $V_d = 0.1$ V); also, $I_g - V_g$ curves (taken at $V_d = 0.1$ V) of TFTs that were activated by front-side green laser irradiation at 2.5 and 2.8 W. (b) Output characteristics of TFTs that were made on CLC poly-Si and activated by FA and front-side green laser irradiation at 2.4–2.8 W.

duces parasitic S/D resistance to a very low value. Therefore, the contribution of R_{on} from parasitic S/D resistance and channel resistance, for green laser-activated TFTs decrease as the laser energy increases and was significantly lower than that of FA-activated TFTs (Fig. 2).

As laser-activation energy increases, the field-effect mobility (μ_{FE}) of green laser-activated TFTs increases markedly from 380 to 620 cm²/V s, which is about double of the FA-activated TFTs, as revealed by the linear transconductance (G_m) curves, which are plotted in Fig. 3(a). The enhancement in the output drive current [Fig. 3(b)] at grain voltage $V_d = 8$ V and gate voltage $V_g = 10$ V was by as much as a factor of 1.3. Under front-side green laser irradiation for transistors with antireflective gate structures, when the laser beam was scanned over the gate structures and the air/S (D) interfaces, inverted laser-energy profiles along channels/junctions/contact regions intrinsically generate and mediate ascendant defect distributions in the microstructures in the S/D regions, across the junctions, toward the channels, generating continuous epilike Si microstructures with fewer grain defects across junctions, as revealed by the cross-sectional transmission electron microscopic image in Fig. 1(c), in response to the enhancement of μ_{FE} .⁶ Additionally, FA-activated TFTs exhibited the lowest parasitic S/D resistance and the smallest μ_{FE} among the present laser (FA)-activated devices such that, in such microchannel TFTs, channel/junction microstructures rather than parasitic S/D resistance dominate electron mobility.

On such an epilike poly-Si, interface trap-state densities (at $\Delta E \sim 0$ eV), which are related to channel roughness, influence the subthreshold slope (S) (Refs. 6 and 17) of the fabricated TFTs. Few extra interface defects are generated because the enhancement of the surface roughness by 40% incident laser-activation energy in the channels is negligible and so, increasing the laser-activation energy slowly reduced S to as low as 130 mV/decade [Fig. 4(a)], which is a better value than 145 mV/decade for FA-activated devices. However, increasing the laser-activation energy initially reduces threshold voltage (V_{th}) to as low as -0.51 V and then increases it to 0.34 V [Fig. 4(a)]. Moreover, a reversal in the deep states of the grain traps at a ΔE of below 0.28 eV for devices was also observed as laser-activation energy was increased to over 2.5 W [Fig. 1(b)]. Hence, the reversal in V_{th}

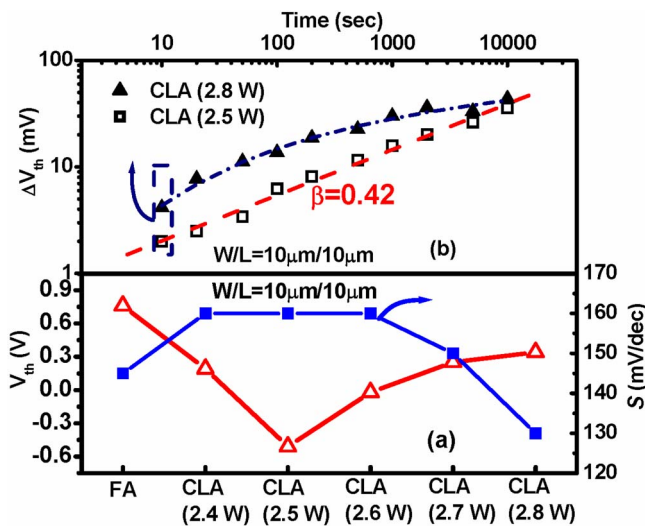


FIG. 4. (Color online) (a) Threshold voltage and subthreshold slope for TFTs that were made on CLC poly-Si, activated by FA and front-side green laser irradiation at 2.4–2.8 W. (b) Degradation of V_{th} of TFTs that were made on CLC poly-Si and activated by front-side green laser irradiation at 2.5 and 2.8 W during HCS.

could not easily be attributed to the increase in the number of interface traps produced by laser activation.

Figure 4(b) plots the V_{th} shift (ΔV_{th}) against the stressing time (t) for laser-activated TFTs during hot-carrier stressing (HCS) ($V_g = 7$ V and $V_d = 14$ V).¹⁷ After HCS for 3 h, very small changes in V_{th} of 42 (35) mV were observed in the TFTs that were activated at a laser-activation power of 2.8 (2.5) W [Fig. 4(b)].¹⁸ In TFTs with antireflective gate structures, front-side green laser activation forms continuous improved epilike Si microstructures with fewer grain defects and with a barely increased number of very few extra interface defects over the entire channel/junction, which markedly inhibited deep-state generation in laser-treated channels/junctions by bias stressing, in response to excellent transistor stability.⁶

Front-side green laser-irradiation likely induces the dehydrogenation of partial Si-rich oxide structures in PECVD SiO_2 to form few defects or Si nanostructures¹⁹ in gate dielectrics and, thus, enhance carrier transportation and charge trapping in gate dielectrics,²⁰ as indicated by the slightly increased gate currents (I_g) of TFTs that had been activated at a high laser-activation energy of 2.8 W [inset of Fig. 3(a)]. The V_{th} degradation of TFTs that was activated at a laser energy of 2.8 W due to HCS typically exhibits a logarithmic time dependence, which reveals charge trapping in gate dielectrics.^{14,21} In contrast, the power-law time dependence of ΔV_{th} with exponents of 0.42 ($\sim t^{0.42}$) for TFTs that were activated at laser energy of 2.5 W due to HCS was observed because the carrier-trapping effect is weaker when fewer de-

fects are formed in the dielectrics by lower laser-energy irradiation such that ΔV_{th} and I_g are smaller [Fig. 4(b)].^{6,17} Hence, slightly worsened gate dielectrics due to front-side laser irradiation enhance charge trapping in dielectrics in response to the reversal in V_{th} .

Antireflective gate structures in self-aligned transistors that were fabricated on green CLC epilike Si active layers were introduced to generate a pertinent inverted laser-irradiation energy profiles along channels/junctions/contact regions. Continuous improved epilike Si microstructures with fewer grain/interface defects over the entire channel/junction and a low parasitic source/drain resistance thus form. Such laser-activated panel transistors thus exhibit extremely high electron mobility and excellent device stability.

The authors would like to thank the National Science Council of the Republic of China, Taiwan for partially supporting this research.

- ¹A. Hara, Y. Mishima, T. Takechi, F. Takeuchi, M. Takei, K. Yoshino, K. Suga, M. Chida, and N. Sasaki, Tech. Dig. - Int. Electron Devices Meet. **2001**, 747.
- ²B. S. Lee, U.S. Patent No. 6703279 (March 7, 2004).
- ³G. K. Giust, T. W. Sigmon, J. B. Boyce, and J. Ho, IEEE Electron Device Lett. **20**, 77 (1999).
- ⁴Q. Zhang, J. Huang, N. Wu, G. Chen, M. Hong, L. K. Bera, and C. Zhu, IEEE Electron Device Lett. **27**, 728 (2006).
- ⁵B. Yu, Y. Wang, H. Wang, Q. Xiang, C. Riccobene, S. Talwar, and M. R. Lin, Tech. Dig. - Int. Electron Devices Meet. **1999**, 509.
- ⁶Y. T. Lin, J. M. Shieh, and C. Chen, IEEE Electron Device Lett. **28**, 790 (2007).
- ⁷D. A. Markle, A. M. Hawryluk, and H. J. Jeong, U.S. Patent No. 6531681 (March 11, 2003).
- ⁸D. Z. Peng, T. C. Chang, H. W. Zan, T. Y. Huang, C. Y. Chang, and P. T. Liu, Appl. Phys. Lett. **80**, 4780 (2002).
- ⁹K. C. Park, S. H. Jung, M. C. Lee, K. C. Moon, and M. K. Han, Tech. Dig. - Int. Electron Devices Meet. **2002**, 573.
- ¹⁰M. Mitsutoshi, O. Tetsuya, T. Hidetada, S. Yukio, I. Mitsuo, and S. Tomohiro, U.S. Patent No. 6573161 (June 3, 2003).
- ¹¹R. Vikas, R. Ishihara, Y. Hiroshima, D. Abe, S. Inoue, T. Shimoda, W. Metselaar, and K. Beenakker, J. Appl. Phys. **45**, 4340 (2006).
- ¹²S. Luan and G. W. Neudeck, J. Appl. Phys. **72**, 766 (1992).
- ¹³G. Fortunato and P. Migliorato, Appl. Phys. Lett. **49**, 1025 (1986).
- ¹⁴Y. T. Lin, C. Chen, J. M. Shieh, Y. J. Lee, C. L. Pan, C. W. Cheng, J. T. Peng, and C. W. Chao, Appl. Phys. Lett. **88**, 233511 (2006).
- ¹⁵K. Y. Choi and M. K. Han, J. Appl. Phys. **80**, 1883 (1996).
- ¹⁶R. F. Wood, J. R. Kirkpatrick, and G. E. Giles, Phys. Rev. B **23**, 5555 (1981).
- ¹⁷Y. T. Lin, C. Chen, J. M. Shieh, and C. L. Pan, Appl. Phys. Lett. **90**, 073508 (2007).
- ¹⁸A. T. Voutsas, D. N. Kouvasos, L. Michalas, and G. J. Papaioannou, IEEE Electron Device Lett. **26**, 181 (2005).
- ¹⁹W. J. Chiang, C. Y. Chen, C. J. Lin, Y. C. King, A. T. Cho, C. T. Peng, C. W. Chao, K. C. Lin, and F. Y. Gan, Appl. Phys. Lett. **91**, 051120 (2007).
- ²⁰M. A. Rafiq, Y. Tsuchiya, H. Mizuta, S. Oda, S. Uno, Z. A. K. Durrani, and W. I. Milne, Appl. Phys. Lett. **87**, 182101 (2005).
- ²¹F. V. Farmakis, J. Brini, G. Kamarinos, and C. A. Dimitriadis, IEEE Electron Device Lett. **22**, 74 (2001).